The 2010 IEEE/RSJ International Conference on
Intelligent Robots and Systems
October 18-22, 2010, Taipei, Taiwan

A Study of Function of Foot's Medial Longitudinal Arch Using Biped Humanoid Robot

Kenji Hashimoto, Yuki Takezaki, Kentaro Hattori, Hideki Kondo,
Takamichi Takashima, Hun-ok Lim, and Atsuo Takanishi

***Abstract*—The humanoid robot, WABIAN-2R, has achieved human-like walking with knee-stretched, heel contact and toe off motions by using a foot mechanism with a passive toe joint. However, the foot structure is different from a human's. In this paper, we describe a new foot mechanism capable of mimicking the human's foot arch structure to figure out the function of the arch structure. Especially, the developed foot mimics the elastic properties of the arch of the human's foot and the change of the arch height during walking. The foot mechanism consists of a passive joint in the internal toe, a passive joint in the external toe, and a joint in the foot arch. We conducted several walking experiments by using WABIAN-2R, and the function of the arch structure is clarified quantitatively. As a result, we confirmed that the arch elasticity could absorb a foot-landing force at the plantar contact phase and the change of the arch height contributed to a strong thrust at the push-off phase.**

I. Introduction

RECENTLY, there are many researches on biped robots. The feet of some biped robots have unique features. For example, ASIMO [1] and HRP-2 [2] have impact absorption mechanisms. WAF-2, the foot system for WL-12RVI, also absorbs impact and contact forces [3]. H6 and H7 have toe joints for walk more quickly in larger steps, extending the active capabilities of the whole body [4]. We also developed some unique foot systems, WS-1 [5] and WS-5 [6], adaptable to uneven terrain.

Just because a human can walk on uneven terrain, it makes no sense for a biped robot to mimic a human's foot structure to realize a stable walk. However, it is important to figure out the function of a human's foot structure. The features of a human's foot structure may be applicable to a robot's foot.

A human foot is anatomically composed of 26 bones excluding sesamoid bone. Considering that an adult human body has 206 bones, a quarter of the bones concentrate in the feet. A human foot has a complex structure, and few mammals, including humans, have a foot arch structure.

There are several theories about the reasons for the existence of the human's foot arch structure. The development of the medial longitudinal arch was a primary step in the evolution of bipedal human gait [7, 8]. This terrestrial modification to the arboreal foot had two major effects. First, it provided the plantar flexors enough mechanical advantage to lift the weight of the body during the stance phase [8, 9]. Second, it provided the foot with the capacity to absorb some of the increased shock caused by upright striding [10]. The transformation of the grasping function of the medial rays of our primate ancestors into the plantigrade propulsive feet of modern human was clearly a seminal event in prehuman evolution [11]. But few theories verified the significance of arch structure quantitatively. The reasons for the existence of the arch structure are still remain to be clarified.

Meanwhile, we have developed a biped humanoid robot named WABIAN-2R (WAseda BIpedal humANoid - No. 2 Refined) to simulate human motion [12, 13] (see Fig. 1). WABIAN-2R has a foot with a passive toe joint and achieves a human-like walk with the knees stretched, heel-contact and toe-off motion. However, the foot of WABIAN-2R is

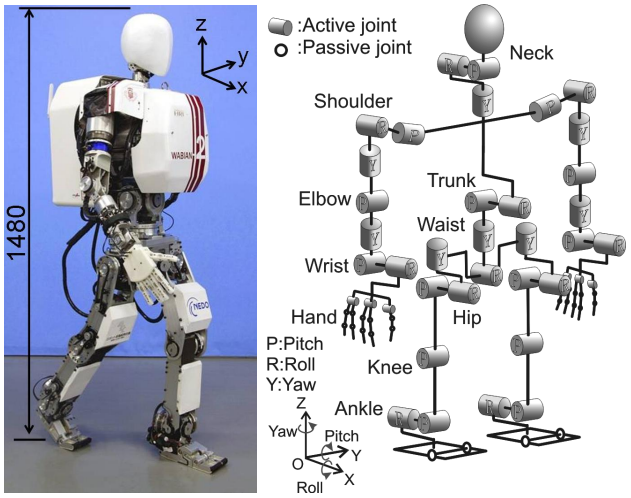

(a) Overview (b) DOF congifuration

Fig. 1. WABIAN-2R.

This study was conducted as part of the Advanced Research Institute for Science and Engineering, Waseda University, and as part of the humanoid project at the Humanoid Robotics Institute, Waseda University. It was also supported in part by Global COE Program "Global Robot Academia" from the Ministry of Education, Culture, Sports, Science and Technology of Japan, Grant-in-Aid for Scientific Research (B) (18360126), SolidWorks Japan K.K., QNX Software Systems, and DYDEN Corporation, whom we thank for their financial and technical support.

Kenji Hashimoto is with the Faculty of Science and Engineering, Waseda University, #41-304, 17 Kikui-cho, Shinjuku-ku, Tokyo 162-0044, JAPAN (e-mail: k-hashimoto@takanishi.mech.waseda.ac.jp).

Yuki Takezaki, Kentaro Hattori, Hideki Kondo are with the Graduate School of Science and Engineering, Waseda University.

Takamichi Takashima is with the College, National Rehabilitation Center for Persons with Disabilities.

Hun-ok Lim is with the Faculty of Engineering, Kanagawa University; and a researcher at the Humanoid Robotics Institute (HRI), Waseda University.

Atsuo Takanishi is with the Department of Modern Mechanical Engineering, Waseda University; and one of the core members of the Humanoid Robotics Institute (HRI), Waseda University.

different from the human's on the point that the foot sole is flat and the foot breadth is wide. In this paper, we aim to figure out the function of human foot in gait. We develop a new biped foot mechanism mimicking a human's foot arch structure and verify the significance of arch structure quantitatively through walking experiments by WABIAN-2R mounted on the new feet.

This paper is organized as follows. Section II describes the details of a new biped foot mechanism mimicking human's foot arch structure. In section III, experimental results and considerations are shown. Section IV provides conclusions and future work.

II. Development of Human-like Foot Mechanism

A. Modeling of Human's Foot Arch Structure

The human foot has three arches; the medial longitudinal arch, the lateral longitudinal arch, and the transversal arch [14]. The chief characteristic of the medial longitudinal arch is its elasticity, due to its height and to the number of small joints between its component parts. The lateral longitudinal arch allows only a limited movement. The most marked features of this arch are its solidity and its slight elevation compared with the medial longitudinal arch. The transversal arch is elastic to follow the unevenness on a ground and cannot keep the arch structure when a large load is applied during walking. The stiffness of the arch was identified at the following four phases in a gait cycle (see Fig. 2);

- Phase I: Heel contact phase
- Phase II: Plantar contact phase
- Phase III: Push-off phase
- Phase IV: Swing phase

In the phase I, the medial longitudinal arch is elastic because a load isn't applied. In the phase II, it provided that the foot can absorb a foot-landing impact force [10]. In the phase III, the toes are extended, and they pull the plantar pads and hence the aponeurosis forward around the heads of the metatarsals, like a cable being wound on to a windlass [15] (see Fig. 3 (a)). As a result, the arch is caused to rise because the distance between the metatarsal heads and the calcaneum is thereby shortened, and the arch becomes the stiffest in a gait cycle. In the phase IV, the arch becomes elastic again because a foot is unloaded. The characteristics of the human's foot are the changes of the elasticity of the medial longitudinal arch with the change of the arch height during walking.

In this research, we approximate the arch structure by a rotational spring and damper as shown in Fig. 3 (b), referring to the Takashima's method [16]. The identified viscoelasticities of k Nm/rad and c Nm/rad^2 show different values in a gait cycle as shown in Table I. In this paper, we focus on only the medial longitudinal arch because the change of its elasticity is much larger than the lateral longitudinal arch and the transversal arch. The foot is classified into the following four parts; the medial toe, the lateral toe, the medial plantar and the ankle-lateral plantar (see Fig. 4).

We set the targets of arch viscoelasticity to the elasticity in the phase II and the phase III. We designed a new foot mechanism as shown in Fig. 5 to mimic the change of the elasticity with the change of the arch height. It consists of a toe axis, an arch axis and a wire that mimics the plantar

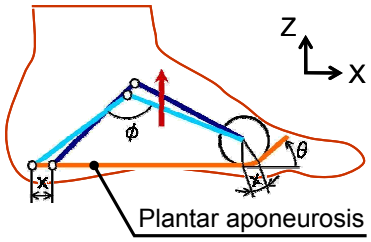

(a) Windlass mechanism [15]

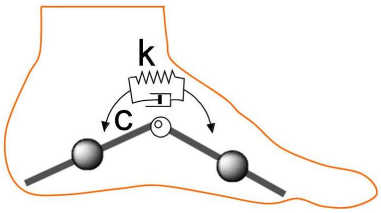

(b) Foot model with a rotational spring-damper

Fig. 3. Modeling of human's foot arch structure.

TABLE I
VISCOELASTICITY AT EACH PHASE [17]

	I	II	III	IV
Elasticity k Nm/rad	19	386	488	-19
Viscosity c Nm/ rad^2	17	24	8	3

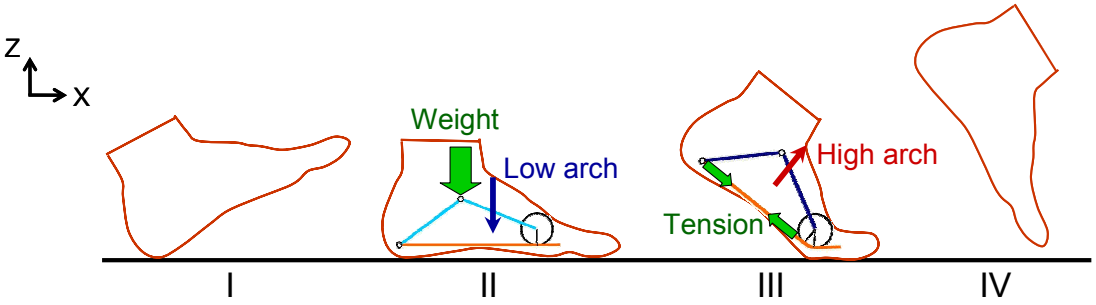

Fig. 2. Transformation of the medial longitudinal arch in a gait cycle.

aponeurosis to realize the windlass mechanism. It has two soft materials to limit the arch movement, and it can realize the change of the arch elasticity during walking.

B. Human-like Foot Mechanism Design

Fig. 6 shows the human-like foot mechanism developed. Its weight is 1.1 kg equal to a human's foot, and its size and the position of each joint axis are determined based on the converted size by the mean size of adult women's feet [18] using the WABIAN-2R's height. It has a medial toe axis, a lateral toe axis and an arch axis. A medial toe axis and an arch axis are connected by a wire which mimics the plantar aponeurosis, and we selected a stainless wire which has a high mechanical strength and a high stiffness. The toes are passive joint as our previous research [13]. The developed foot also mimics the change of the arch height in the phase II and the phase III by applying a windlass mechanism as shown in Fig. 3 (a). The selection of two soft materials attached to the arch is described in the next section.

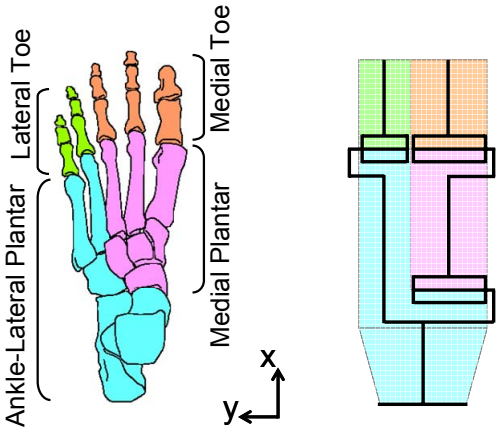

(a) Foot skeleton model (b) 3-DOF model

Fig. 4 Foot model.

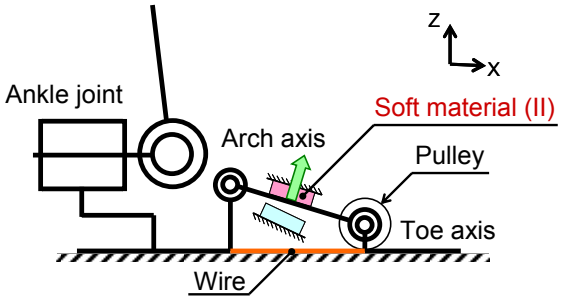

(a) Medial longitudinal arch at phase II

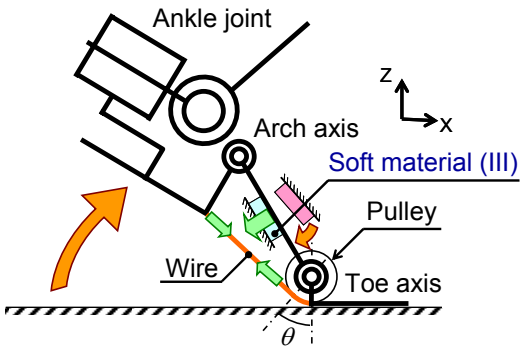

(b) Medial longitudinal arch at phase III

Fig. 5. Joint configuration.

C. Medial Longitudinal Arch Compliance Mimesis

The developed foot mechanism mimics the rotational spring constant by attaching a soft material between the foot frame and the stopper. The soft material is selected through compression tests using a universal testing machine as shown in Fig. 7. A compressive load is applied to the developed foot with the universal testing machine, and a rotational spring constant is calculated from the moment about the arch axis.

To calculate the rotational spring constant k_{II} in the phase

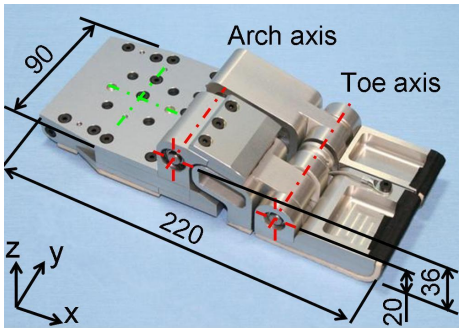

(a) Photograph

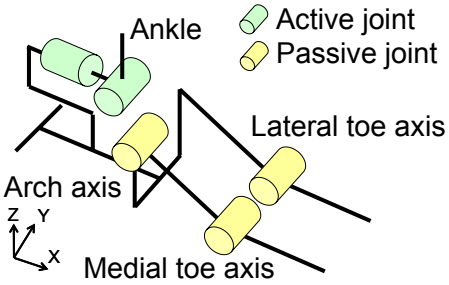

(b) DOF configuration

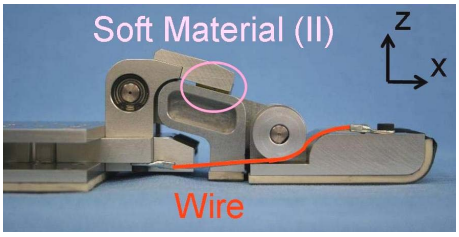

(c) Medial longitudinal arch at phase II

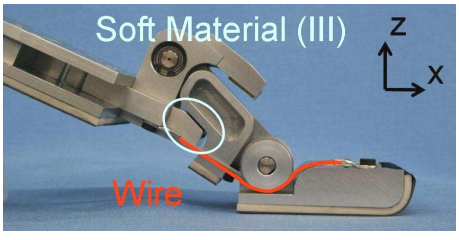

(d) Medial longitudinal arch at phase III

Fig. 6. Human-like foot mechanism with the medial longitudinal arch.

II, we used the model as shown in Fig. 8. The arch rotation angle $\Delta\phi(t)$ rad and the moment $M(t)$ kNmm about the arch axis can be calculated from the measured vertical displacement $\Delta z(t)$ mm and the vertical force $F(t)$ kN as follows;

$$\Delta z(t) = l_1 \sin\phi_0 - l_1 \sin\left(\phi_0 - \Delta\phi(t)\right) \quad (1)$$

$$M(t) = l_1 F(t) \cos\left(\phi_0 - \Delta\phi(t)\right) \quad (2)$$

where l_1 is the distance between the arch axis and the toe axis, and ϕ_0 is the initial arch angle.

The rotational spring constant $k_{II}(t)$ Nm/rad in the phase II is calculated from the above equations as follows;

$$k_{II}(t) = \left(M(t+1) - M(t)\right) / \left(\Delta\phi(t+1) - \Delta\phi(t)\right) \quad (3)$$

After conducting experiments repeatedly by changing kinds and thickness of soft material, we selected a polyurethane rubber whose Shore hardness is Shore A 30 with 10 mm thickness as the soft material in the phase II.

To calculate the rotational spring constant k_{III} in the phase III, a compressive load is applied to the developed foot with the universal testing machine as shown in Fig. 9, and we used the model as shown in Fig. 10. The relational expression among the arch rotation angle $\Delta\phi(t)$ rad, the moment $M(t)$ kNmm about the arch axis, the measured vertical displacement $\Delta z(t)$ mm and the vertical force $F(t)$ kN is described as follows;

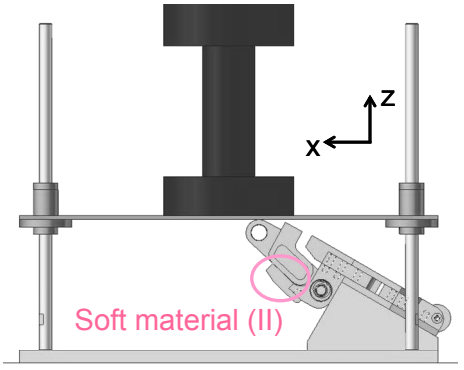

Fig. 7. Experimental setup for the phase II.

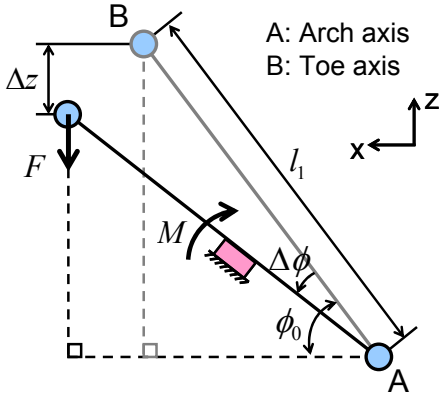

Fig. 8. Modeling of the foot for the phase II.

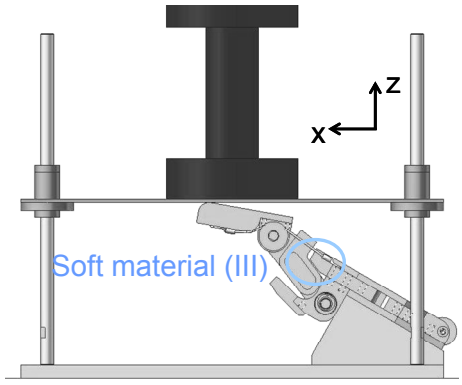

Fig. 9. Experimental setup for the phase III.

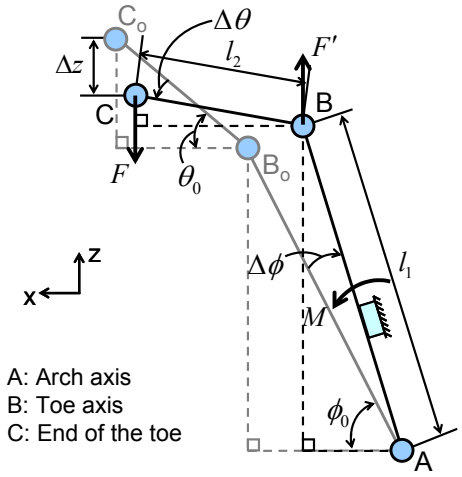

(a) $M(t)$ and $\Delta\phi(t)$

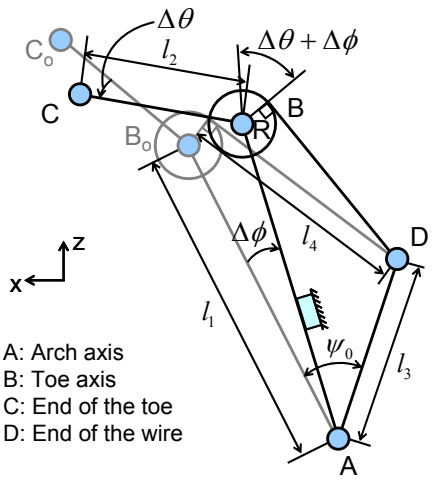

(b) $\Delta\phi(t)$ and $\Delta\theta(t)$

Fig. 10. Modeling of the foot for the phase III.

TABLE II
PARAMETERS

l_1 mm	l_2 mm	l_3 mm	l_4 mm	R mm	ψ_0 deg
64.8	51.8	35.4	46.0	9.25	45.0

$$\Delta z(t) = l_1\left\{\sin\phi_0 - \sin\left(\phi_0 - \Delta\phi(t)\right)\right\} + l_2\left\{\sin\theta_0 - \sin\left(\theta_0 - \Delta\theta(t)\right)\right\} \quad (4)$$

$$M(t) = l_1 F(t)\cos\left(\phi_0 + \Delta\phi(t)\right) \quad (5)$$

The following equation can be obtained from the law of cosines for a triangle ADR as shown in Fig. 10 (b);

$$\cos\left(\psi_0 - \Delta\phi(t)\right) = \frac{l_1^2 + l_3^2 - \left\{l_4 - R\left(\Delta\theta(t) + \Delta\phi(t)\right)\right\}^2 - R^2}{2l_1 l_3} \quad (6)$$

where all the parameters of l_1, l_2, l_3, l_4, R and ψ_0 are given as shown in Table II.

The moment $M(t)$ is calculated by solving (4), (5) and (6), and the rotational spring constant k_{III} in the phase III is also calculated as (3). However, the rotational spring constants had a constant value as 60 Nm/rad, and we could not find significant differences of rotational spring constants among soft materials. This is because a stainless wire mimicking the plantar aponeurosis is "a stranded wire" and it can be stretched at a low-load condition. The soft material for the phase III cannot be compressed enough due to the stretch of the stainless wire. To mimic the rotational spring constant k_{III}, a wire which is hard to be stretched should be selected, or the foot mechanism itself should be reconsidered.

However, the developed foot mimics the rotational spring constant at the phase II and the change of the arch height during walking. It is possible to verify the shock absorbing function at the phase II which is explained as a hypothesis about the reason for the existence of the arch structure in ergonomics field [10]. It is also possible to verify the function of the windlass mechanism related to the change of the arch height. So we conducted some experiments described in the next chapter.

III. Experimental Tests and Consideration

A. Verification of Walking with Human-like Foot Mechanism

Because the breadth of the developed foot is as narrow as 90 mm, we must confirm whether a humanoid biped robot, WABIAN-2R can walk with the knees stretched, heel-contact and toe-off motion. The human-like foot mechanism was attached to WABIAN-2R, and forward walking experiments were conducted with a step length of 450 mm/step and a walking cycle of 1.0 s/step. We applied a polyurethane rubber with the hardness of Shore A 30 and the thickness of 10 mm to the soft material for the phase II. We tentatively applied a polyurethane rubber with the hardness of Shore A 70 and the thickness of 5 mm to the soft material for the phase III, and the medial longitudinal arch is transformed by the stainless wire. Then the rotational spring constant in the phase III is 60 Nm/rad. As shown in Fig. 11, WABIAN-2R mounted on the human-like foot mechanism realized a stable walk with the knees stretched, heel-contact and toe-off motion.

B. Consideration of Function of Medial Longitudinal Arch

We compared the vertical ground reaction forces when a polyurethane rubber (Shore A 30 and 10 mm thickness) is attached to the arch and when a fixation part is attached to the arch (Fig. 12). When a polyurethane rubber is attached to the arch, the medial longitudinal arch is movable and the arch height changes. When a fixation part is attached to the arch, the medial longitudinal arch is fixed.

Fig. 13 shows the ground reaction force in a gait cycle. At the beginning of the phase II, the foot-landing force with movable-arch condition was smaller than that with fixed-arch

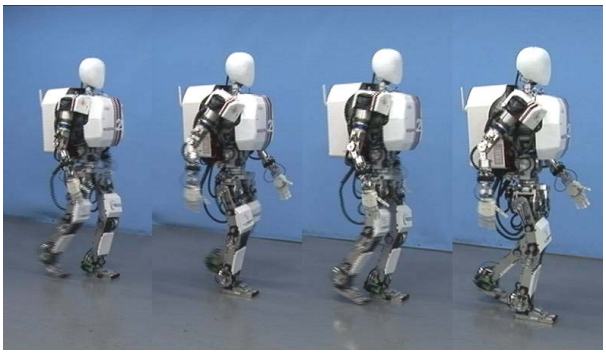

Fig. 11. Walking experiment with human-like foot mechanism developed. The walking cycle is 1.0 s/step and the step length is 450 mm/step.

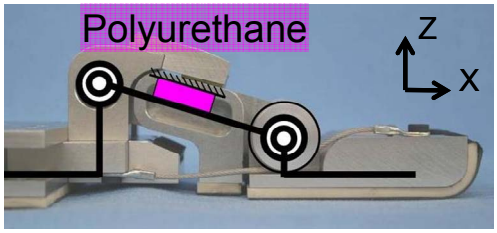

(a) Medial longitudinal arch is movable

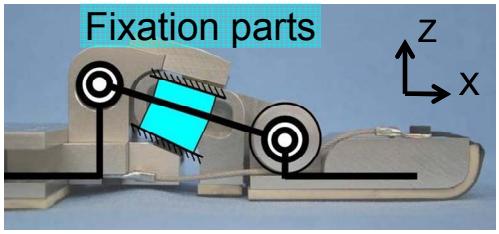

(b) Medial longitudinal arch is fixed by fixation parts

Fig. 12. Experimental condition.

condition. We can find the significant differences ($p<0.05$) as shown in Fig. 14. So, we confirmed that the foot can absorb a foot-landing force by the elastic properties of the medial longitudinal arch.

We can also find that the ground reaction force with movable-arch is larger than that with fixed-arch at the end of the phase II. It is considered that the windlass mechanism which causes the change of the arch height contributes to this strong thrust at the push-off phase. If the heel point is fixed in Fig. 3, the toe position moves to the left with elevation of the arch height, and this movement contributes to the strong thrust at the push-off phase.

IV. Conclusions and Future Work

To clarify the function of the foot arch structure, we developed a new human-like foot mechanism that mimics the changes of the elasticity of the medial longitudinal arch with the change of the arch height during walking. As experimental results using a biped humanoid robot, WABIAN-2R mounted on the new human-like foot mechanism, we confirmed that the arch elasticity could absorb a foot-landing force at the plantar contact phase and the windlass mechanism which caused change of the arch height contributed to a strong thrust at the push-off phase.

At the present stage, the mimesis of the elasticity at the phase III has not completely realized. Therefore, we will improve the human-like foot mechanism and continue to research to clarify the function of the arch structure quantitatively.

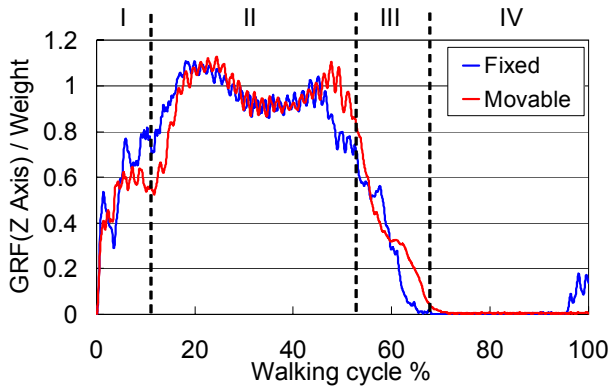

Fig. 13. Vertical ground reaction force in a gait cycle. GRF with movable-arch is smaller than GRF with fixed-arch at the beginning of the phase II. GRF with movable-arch is larger than that with fixed-arch at the end of the phase II.

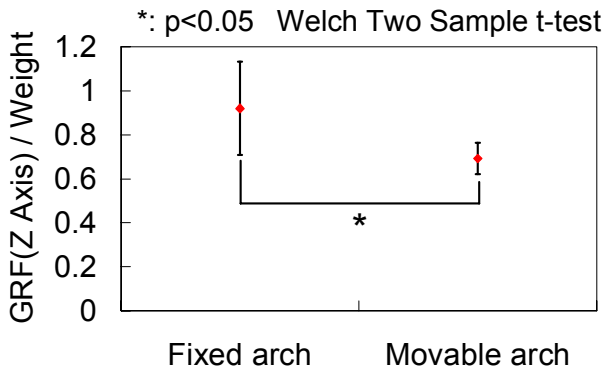

Fig. 14. Welch two sample t-test of ground reaction forces at the beginning of phase II.

References

[1] M. Hirose, Y. Haikawa, T. Takenaka, and K. Hirai, "Development of Humanoid Robot ASIMO," Proc. of the IEEE/RSJ International Conference on Intelligent Robots and Systems , Workshop2, 2001.

[2] K. Kaneko, et al., "Design of Advanced Leg Module for Humanoid Robotics Project of METI," Proc. of the IEEE International Conference on Robotics and Automation, pp. 38-45, 2002.

[3] J. Yamaguchi, A. Takanishi, and I. Kato, "Experimental Development of a Foot Mechanism with Shock Absorbing Material for Acquisition of Landing Surface Position Information and Stabilization of Dynamic Biped Walking," Proc. of the IEEE International Conference on Robotics and Automation, pp. 2892-2899, 1995.

[4] K. Nishiwaki, S. Kagami, J. Kuffner, M. Inaba, and H. Inoue, "Humanoid 'JSK-H7': Reserch Platform for Autonomous Behavior and Whole Body Motion," Proc. of the Third IARP International Workshop on Humanoid and Human Friendly Robotics, pp. 2-9, 2002.

[5] K. Hashimoto, Y. Sugahara, H. O. Lim and A. Takanishi, "New Biped Foot System Adaptable to Uneven Terrain," Journal of Robotics and Mechatronics, Vol. 18, No. 3, pp. 271-277, 2006.

[6] K. Hashimoto, et al., "New Foot System Adaptable to Convex and Concave Surface," Proc. of the IEEE International Conference on Robotics and Automation, pp.1869-1874, 2007.

[7] M. H. Day and J. R. Napier., "Fossil foot bones," Current Anthropology, Vol. 6, No. 4, pp. 419-420, 1965.

[8] D.J. Morton., "Evolution of the longitudinal arch of the human foot," Journal of Bone Joint Surgery, Vol. 6, pp. 56-90, 1924.

[9] A. H. Schultz., "Relatives between the lengths of the main parts of the foot skeleton in primates," International Journal of Primatology, Vol. 1, pp. 150–171, 1963.

[10] R. F. Ker, M. B. Bennett, S. R. Bibby, R. C. Kester, and R. McN. Alexander, "The spring in the arch of the human foot," Nature, Vo. 325, pp. 147–149, 1987.

[11] M. Harris, "Our Kind: Who We Are, Where We Came From, Where We Are Going," Herper Perennial, 1990.

[12] Y. Ogura, H. Aikawa, K. Shimomura, H. Kondo, A. Morishima, H. O. Lim and A. Takanishi, "Development of a Humanoid Robot WABIAN-2," Proc. of the 2006 IEEE International Conference on Robotics and Automation, pp. 76-81, 2006.

[13] Y. Ogura, K. Shimomura, H. Kondo, A. Morishima, T. Okubo, S. Momoki, H. O. Lim and A. Takanishi, "Human-like Walking with Knee Stretched, Heel-contact and Toe-off Motion by a Humanoid Robot," Proc. of the 2006 IEEE/RSJ International Conference on Intelligent Robots and Systems, pp. 3976-3981, 2006.

[14] I. A. Kapandji, "The Physiology of the joints: Lower limb, Volume 2," Churchill Livingstone, 1988.

[15] J. H. Hicks, "The mechanics of the foot: II. The plantar aponeurosis and the arch," Journal of Anatomy, Vol. 88, pp. 25-30, 1954.

[16] T. Takashima, H. Fujimoto, and A. Takanishi, "Determination of the longitudinal arch moment of the human foot complex during gait: inverse dynamics model analysis," Transactions of the Japan Society of Mechanical Engineers. C, Vol. 68, No. 672, pp. 2425-2430, 2002. (in Japanese)

[17] T. Takashima, H. Fujimoto, and A. Takanishi, "Analysis of the human foot arch viscoelasticity using the simple model of the arch support elements," Transactions of the Japan Society of Mechanical Engineers. C, Vol. 69, Vol. 685, 2003. (in Japanese)

[18] M. Kouchi and M. Mochimaru, "AIST Research Information Database (http://riodb.ibase. aist.go.jp/riohomee.html)," H16PRO287, 2005.